# Computer Aided Modeling and Simulation of Artificial Knee Joint in Biomedical Applications

**R.P.Thirumurugan**

*Abstract*— **Artificial Knee Joint dynamic models capable of forecasting muscle forces and joint contact pressures simultaneously would be valuable for studying clinical issues related to knee joint degeneration and restoration. Recent three-dimensional Artificial Knee Joint models are either static with deformable contact or dynamic with rigid contact. This investigation gives an efficient methodology for replacing Mobile bearing dynamic simulation methods with a deformable contact knee model. The recent implementation accommodates natural or artificial Knee joint models, small or large strain contact models, and linear or nonlinear material models. Applications are presenting for static analysis or dynamic simulation of a natural knee model created from MRI and CT data and dynamic simulation of an artificial knee model created from manufacturer's CAD. This investigation can be replaced the mobile bearing from Polyethylene to PMMA with PLLA by copolymer property. Mostly Polyethylene and PMMA used in Artificial Knee Joint. Its stability is in 10 to 12 years only. It was worn out. It can be prevented by replacing of copolymer material of PMMA and PLLA for purpose of stability and more wear resistance and withstand load. This investigation is focused on the force and stress analysis in replacement of mobile bearing in Artificial Knee Joint with 3D modeling in PRO-E and analysis in ANSYS.**

*Index Terms*— **Artificial Knee Joint dynamic models, PMMA, PLLA, 3D modeling and analysis**

## I. INTRODUCTION

The knee joint is subjected to a complex combination of rolling, sliding and rotational movement resulting in a high load applied to the polymer sliding counterpart. Wear by abrasion is one of the main causes for failures of artificial knee joints and causes for this wear are listed below:

Wearing out of the knee joint due to age, Lack of blood flow to the lower end of the thigh bone and it is resulting in weakened and dead bone tissue and moderate bow-legged, knock-kneed or bending abnormality of the knee, wearing out of the knee joint due to damage sustained from a physical injury. Successful mobile bearing transplantation may depend on accurate sizing. Mobile bearing size is currently determined by measuring a combination of bony landmarks and soft-tissue insertion points through images obtained radiographically or by magnetic resonance imaging (MRI). The literature widely reports inaccuracy in size resulting from radiographic errors in magnification, erroneous identification of bony landmarks, and difficulty in differentiating soft-tissue and bone interface. In our mobile bearing transplantations we have observed that when the height and weight of the recipient matched those of the donor, the meniscal size appeared to be a match at surgical implantation; we designed this study to confirm this observation. New and existing Mobile bearing modeling can be explained in this investigation. In modeling, analysis, simulation and system, the software plays a powerful role in functionality and efficiency. In the R&D of custom-made artificial knee, Pro/E constructs the geometric model of knee joint and it analysis with ANSYS.

### 1.1 Objective

The objective of this study is to replace the existing material in to new thermoplastic material for new mobile bearing in artificial knee joint.

To capable of forecasting muscle forces and joint contact pressures simultaneously would be valuable for studying clinical issues related to knee joint degeneration and restoration.

To analysis an efficient methodology for replacing Mobile bearing dynamic simulation methods with a deformable contact knee model.

To obtain good result from in this investigation by using CAD software tools.

### 1.2 Scope

The recent implementation accommodates natural or artificial Knee joint models, small or large strain contact models, and linear or nonlinear material models. In various biomedical industries are to be need for rectifying most wear failure of artificial knee mobile bearing. The recent applications are presenting for static analysis or dynamic simulation of a natural knee model created from MRI and CT scan data and dynamic simulation of an artificial knee model can be created from manufacturer's CAD in Biomedical industries.

### 1.3 Justification for the selection of project work

Mostly Polyethylene used in Artificial Knee Joint. The Polyethylene stability is in 8 to 10 years only. It was worn out. It can be prevented by replace of copolymer material of PMMA and PLLA for purpose of stability and more wear resistance to withstand load. In this investigation is focused on stress and strength analysis in replacement of mobile bearing in Artificial Knee Joint by using 3D modeling in PRO-E and analysis in ANSYS. Recent three-dimensional Artificial Knee Joint models are either static with deformable contact or dynamic with rigid contact.

Manuscript received Dec 15, 2016

**R.P.Thirumurugan,** Assistant Professor**,** Department of Mechanical Engineering, EASA College of Engineering & Tech

## II. SYSTEM ANALYSIS

### 2.1 Existing system

Ultra-high molecular weight polyethylene (UHMWPE) knee bearing components was carried out on a knee implants of meniscus. Tibial components for the knee simulator were gamma-sterilized, implantable components taken from manufacturing inventory. In this investigation is taken already existing fixed polyethylene mobile bearing. The existing material is shown in fig.1.

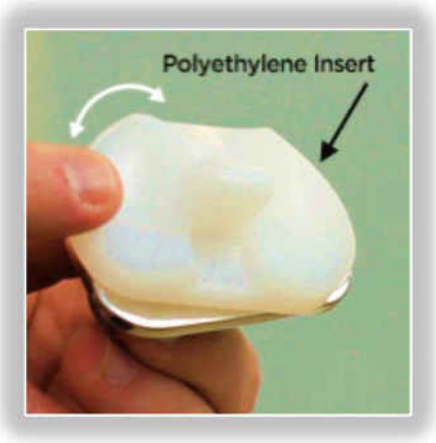


Fig.1: The existing polyethylene mobile bearing.

#### 2.1.1 Drawbacks of the existing system

Mostly Polyethylene used in Artificial Knee Joint. The Polyethylene stability is in 10 to 12 years only. It was worn out. Polyethylene has high thermal expansion. It leads to wear due to weak property of polyethylene. The rolling and sliding load conducts in between tibia and femur to wear in the polyethylene. The knee joint is subjected to a complex combination of rolling, sliding and rotational movement resulting in a high load applied to the polyethylene sliding counterpart. Wear by abrasion is one of the main causes for failures of artificial knee joints. Wear failure of polyethylene is shown in fig.2.

Fig.2: Polyethylene wear.

### 2.2 Proposed system

This can be rectified by combination of PMMA and PLLA blends, copolymer material. It has less thermal expansion. It leads to less wear and good strength of mobile bearing comparing with polyethylene.

### 2.3 Feasibility study

#### *2.3.1 Economical feasibility*

This is inner human body implant. So it is required high care and cost is moderate.

#### *2.3.2 Operational feasibility*

This is biocompatible property of inner human body.so it has suitable operational feasibility in inside human body

#### *2.3.3 Technical feasibility*

In this system has technological wise to fulfill the model and strength such as dimensional modification, material modification, modulus and wear simulation technique.

### 2.4 Methodology

The methodology of the work as follows in fig.3. This methodology is mainly to describe the stress analysis of two methods (existing bearing and new bearing) by using PEO-E and ANSYS. We are comparing to result the best one. In this investigation, work is focusing on collection of data, selection of material and 3D modeling of existing and new mobile bearing by using PRO-E. The remaining meshing, analysis and comparison are planned to carry on future work of project by using ANSYS analysis.

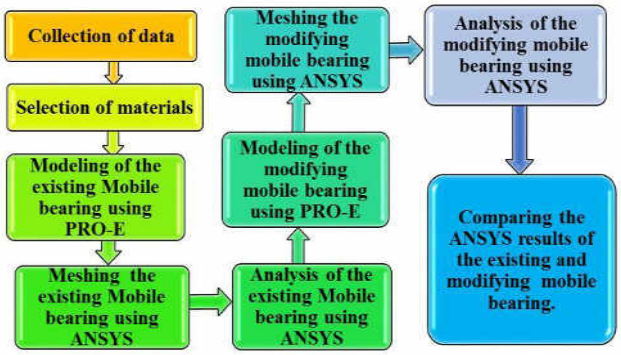


**Fig.3: Methodology of the work.**

### 2.5 System specification

#### *2.5.1 Hardware Requirements*

Manufacturer: Driver pack solution Model: HCL info systems ltd.
Processor: Intel® Pentium® cpu@2.10GHZ RAM: 2GB
System type: 32-bit operating system.

#### *2.5.2 Software requirements*

Operating software: windows 7 ultimate, service pack1.
Design software: PRO/Engineer wildfire 5.0 software.
Analysis software: ANSYS 13.

### 2.6 Software description

3D model of existing mobile bearing and new mobile bearing is performed by PRO/Engineer wildfire 5.0 software. Fundamentals discusses the basic tasks in using Pro/ENGINEER, such as collaboration, managing data,

working with the user interface, working with the model, and so on. Analysis of existing mobile bearing and new mobile bearing is performed by ANSYS 13 software. Fundamentals discusses the basic tasks in using Pro/ENGINEER and ANSYS 13, such as collaboration, managing data, working with the user interface, working with the model, and so on.

## III. DESIGN PROCEDURE

### 3.1 The Knee anatomy

The knee anatomy is shown in fig.4.

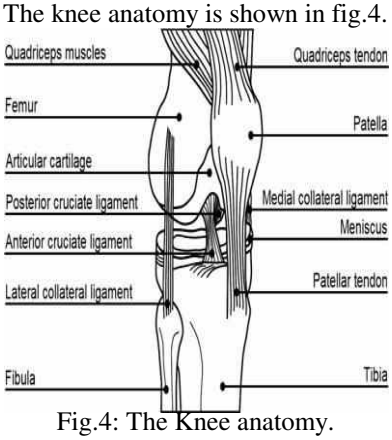


Fig.4: The Knee anatomy.

The Knee joint is the largest, strongest and most complex joint structure in our human body. It has three bones such as femur, tibia and patella. It has three compartments such as Medial, Lateral and Patellofemoral. It has four Ligaments such as MCL, LCL, ACL and PCL. It has two Menisci such as medial and lateral. It has one Articular Cartilage.

### 3.2 Problem definition

Knee joints are identified Right and Left Knee joint before the problem definition. The Right and Left Knee joint is shown in fig.5.

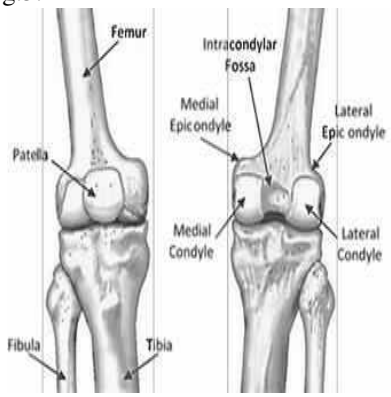


**Fig.5: a) Right Knee joint b) Left Knee joint**

Femur is a top part of knee joint to withstand body load. This part is shown in fig.6.


**Fig.6: Femur (Thighbone)**

Tibia is a bottom part of Knee joint to withstand ground reaction load. This part is given below in fig.7.


Fig.7: Tibia (shinbone).

Patella is a Knee cap. It is a locking part of Knee joint. It is given below in fig.8.


Fig.8: Patella (Knee Cap).

These are stabilized by various ligaments. Meniscus is a middle part in between femur and tibia. It has two parts such as Medial and Lateral. It is shown in fig.9.

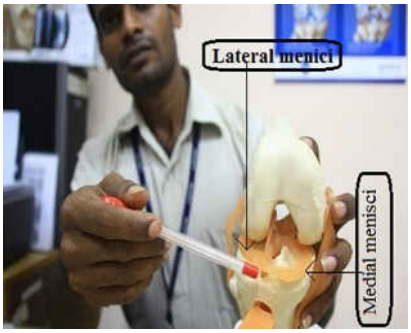


Fig.9: Lateral and Medial menisci

It acts as shock absorber and friction resistance. Meniscus is a main role of this investigation part. Investigation part is shown in fig.10.

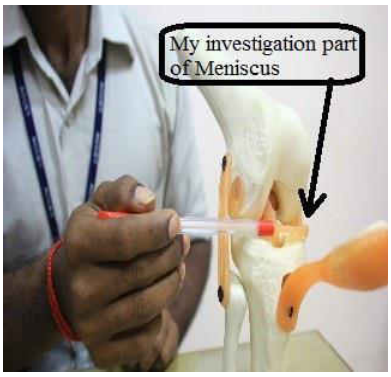

Fig.10: Investigation part of meniscus.

Already existing polyethylene can be replaced by combination of PMMA with PLLA copolymer material.

### 3.3 Collection of data

The MRI-based meniscal sizing of 111 patients (63 male and 38 female; mean age, 44 years [range, 15 to 76 years]), totaling 147 menisci (87 lateral and 60 medial), was compared with the height and weight of each patient. MRI scans were obtained with a 1.0Tesla MRI system (ONI Medical Systems, Wilmington, MA). Sizing was performed by an independent musculoskeletal MRI radiologist using radiographic and MRI bony landmarks and insertion points (Fig.11).

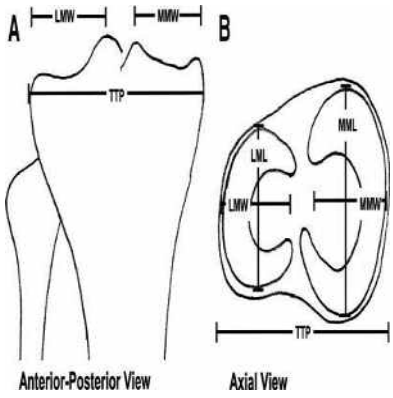


**Fig.11: Meniscus size by MRI method.**

The method of meniscal sizing by MRI was performed as established in the literature survey. In my investigation, collection of data from the MRI-based meniscal sizing of 5 patients was compared and it compared with above survey most suitable of size of meniscal. The X-Ray of pre implant of defect meniscus and post implant of knee joint is indicated below. (Fig.12 to 15).

**Pre implant:**

Fig.12: Pre implant model-I.


**Fig.13: Pre implant model II.**

In literature survey, Statistical methods include nonparametric Pearson correlation (r) between MRI-based lateral meniscal width, lateral meniscal length, medial meniscal width, medial meniscal length, total tibial plateau width, and patient height, weight, and body mass index (BMI). Significance at the P 0.05 level was used.

**Post implant:**

Fig.14: Post implant models I.

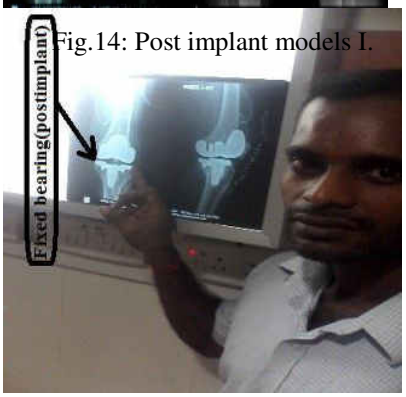


Fig.15: Post implant model II.

Current imaging techniques extract meniscal dimensions from bony landmarks. Height, weight, and gender are easily obtained variables and are correlated with bony landmarks and, to a lesser degree, meniscal dimensions. Statistical power is compromised by each stratification of the data because the power is dependent on sample size; however, these exploratory statistics establish promising correlations between height, weight, gender, and meniscal size that can be extended to estimating meniscal size. Practically, this correlation has been supported in our parallel clinical experience of more than 100 meniscus transplantations using gender, height, and weight as the sizing methodology. Height, weight, and gender should be considered by both tissue banks and surgeons as a fast and cost-effective method for meniscal sizing.

**Table.1: Correlations of Height, Weight, Meniscal Size, and Total Tibial Plateau Width for 10 Menisci**

| Sizes | Height | Weight | TTP | MMW | MML | LMW | LML |
|---|---|---|---|---|---|---|---|
| Height | 1.0000 | 0.6766 | 0.7092 | 0.5966 | 0.5164 | 0.5178 | 0.5278 |
| Weight | | 1.0000 | 0.6723 | 0.6132 | 0.4563 | 0.3872 | 0.4734 |
| TTP | | | 1.0000 | 0.7734 | 0.7125 | 0.7345 | 0.7352 |
| MMW | | | | 1.0000 | 0.6745 | 0.0895 | 0.0098 |

| | | | | | | | |
|---|---|---|---|---|---|---|---|
| MML | | | | | 1.0000 | 0.0567 | 0.2034 |
| LMW | | | | | | 1.0000 | 0.4799 |
| LML | | | | | | | 1.0000 |

The above correlation is to form line of equation. It is given below.

**Table.2: Line equations of Group**

| Group( Height v TTP) | No. of Menisci | Line Equation | Pearson Correlation (r) |
|---|---|---|---|
| All | 10 | y = 0.1830x + 2.0831 | 0.65 |
| Men | 4 | y = 0.2461x + 1.6582 | 0.48 |
| Women | 6 | y = 0.1135x + 2.9999 | 0.40 |

Female patients generally present with smaller total tibial plateau widths than male patients. The variance observed at any given height can be adjusted by considering weight. Height versus Total Tibial Plateau Width: Gender Stratification;

This is explained in suitable graph with 10 series of samples. The height vs. TTP width is shown in fig.16.

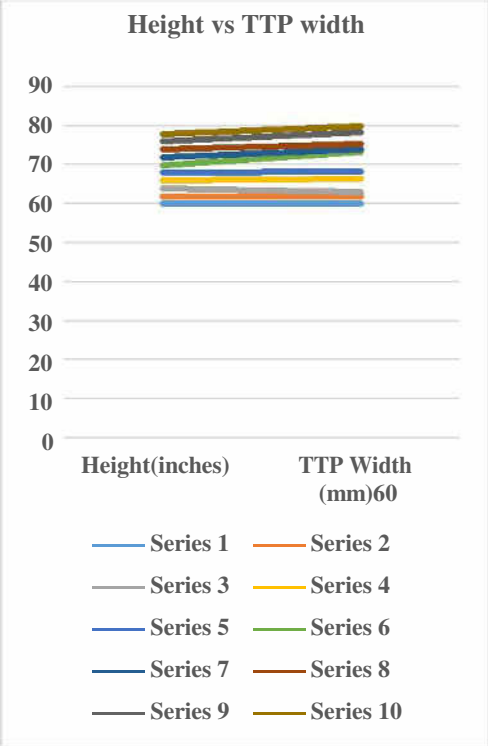


**Fig.16: Height vs. TTP width.**

**Table.3: Comparison of High-BMI groups and low-BMI groups.**

| Sizes vs. Groups | Measurement (mean) | | |
|---|---|---|---|
| | Low-BMI Groups | High-BMI Groups | P value |
| LMW (mm) | 28.4 (0.43) | 29.8 (0.43) | .0435 |
| LML (mm) | 34.8 (0.46) | 37.0 (0.43) | .0022 |
| MMW (mm) | 29.5 (0.32) | 32.2 (0.43) | .0005 |
| MML (mm) | 43.8 (0.53) | 45.1 (0.46) | .0899 |
| TTP (mm) | 73.7 (0.55) | 78.4 (0.65) | .0028 |

High-BMI groups present with significantly larger meniscal dimensions than low-BMI groups at any given height for all dimensions with the exception of medial meniscal length.

***3.3.1 Obtained data:***

The above statistical method give to take the average mobile bearing size based on height, weight and gender menisci.

GENDER WITH AGE: Male/female-35 to 80 Yrs. (Female-50 Yrs.)

HEIGHT: 150 to 190 cm (170 cm).

WEIGHT: 50 to 150 kg (150kg).

PHYSICAL SHAPE: Obesity and athletics.

**3.4 Selection of materials**

In this section is explained about design and material wise to select the new specimen and to compare with existing system.

***3.4.1 Existing Design and Material***

The Design of existing mobile bearing is fixed bearing and equal dimensions of lateral and medial area. It has less conducting area and more material accumulation.

LML- 45.1mm.
LMW- 32.2mm.
MML- 45.1mm.
MMW- 32.2mm.
TTP- 80.8mm. Vertical sliding post- 19mm. M4x7 - 4 holes.

**Polyethylene material**

It is a polymer of ethylene, CH2-CH2, having the formula (-CH2-CH2-)n, and it is produced at high pressures and temperatures in the presence of any one of several catalysts, depending on the desired properties for the finished product. Polyethylene is resistant to water, acids, alkalis, and most solvents. Polyethylene is classified into several different categories based mostly on its density and branching. Ultra high molecular weight polyethylene (UHMWPE) is mostly using in Knee implants. Tensile strength is 10 to 30 MPa. Tensile modulus is 1 to 1.5 GPa. Density is 0.941 g/cm$^3$ and Poisson's Ratio (μ) is 0.4. Tensile modulus is derived from polyethylene test specimen by tensile testing method.

**3.4.2 Modifying design and newly formed material**

The Design of modifying mobile bearing is movable or rotating and minimum dimension of lateral than

medial area. It has more conducting area and less material accumulation.

**PMMA- POLY METHYL METHACRYLATE;**

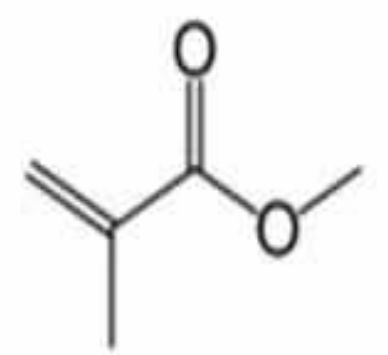

**Fig.17: PMMA molecular formula.**

PMMA is a strong and lightweight material. It has a density of 1.17–1.20 g/cm$^3$. PMMA ignites at 460 °C (860 °F). PMMA has a maximum water absorption ratio of 0.3–0.4% by weight. Tensile strength decreases with increased water absorption. Its coefficient of thermal expansion is relatively high at (5–10) $\times 10^{-5}$ K$^{-1}$. PMMA swells and dissolves in many organic solvents. PMMA has a good degree of compatibility with human tissue. PMMA has a Young's modulus between 1.8 and 3.1 GPa, which is greater than that of natural bone (around 14 GPa for human cortical bone).

**POLY L- LACTIDE: (PLLA)**

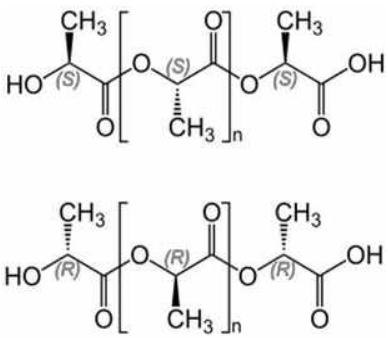

**Fig.18: PLLA molecular formula.**

Molecular formula - (C3H4O2)n. Polylactic acid or polylactide (PLA) is a thermoplastic aliphatic polyester derived from renewable resources, such as corn starch (in the united states), tapioca roots, chips or starch (mostly in Asia), or sugarcane (in the rest of the world).

**Properties:**

Density: 1210-1430 kg/m$^3$, Melting point: 150-160$^0$c, Insoluble in water. Poly-L-lactide (PLLA) is the product resulting from polymerization of L, L-lactide (also known as L-lactide). PLLA has a crystallinity of around 37%, a glass transition temperature between 60-65 °C, a melting temperature between 173-178 °C and a tensile modulus between 2.7-16 GPa. Heat resistant PLA can withstand temperatures of 110 °C. PLA is soluble in chlorinated solvents, hot benzene, tetrahydrofuran, and dioxane.

**PMMA-POLY METHYL METHACRYLATE blends with POLY L- LACTIDE (PLLA);**

Bio based PLLA and petro-based poly methyl methacrylate (PMMA) is proposed in order to tune morphologies and properties of resulting blends upon either a solvent-casting method or a twin-screw extrusion. The solvent-casting process proved only able to produce immiscible blends with matrix–droplet or co-continuous morphologies in function of the blend composition and the immiscibility–miscibility transition is not observed for temperature lower than 250 °C

**Preparation of the PMMA-PLLA Copolymer:**

We added Br-PLLA-Br, cuprous chloride (CuCl), 2, 2-bipyridyl (bpy), MMA (1:4:8.5:2000, mol), vacuum pumped repeatedly, sealed the ampule, and put it in an 80 ˚C oven. After a certain amount of time, we removed the ampule, scraped it, and put the product and glass fragments into a clean conical beaker. We added DCM to dissolve the product and filtered out the glass fragments. We concentrated the product under reduced pressure, added 30 ml alcohol to precipitate the product, washed it five times until the wash solution became colorless, collected the product, and vacuum dried it to a constant weight to obtain the crude product

**PMMA-PLLA-PMMA.**

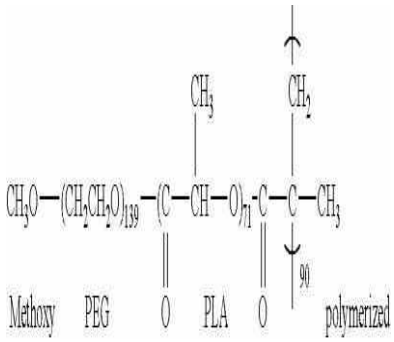


**Fig.19 PMMA-PLLA molecular formula**

**Properties:**

The copolymer's Tg increased from 58 ˚C to 107 ˚C. The PLLA and PMMA blocks are highly biocompatible. New model has a good degree of compatibility with human tissue. The initial decomposition temperature increased from 243 ˚C to 350 ˚C.

Tensile modulus increased 22% and fracture strength 15%. Flexural modulus was 7-8% above the proportional value. Dynamic measurements at the glass transition revealed enhanced modulus (storage) around the phase inversion where the modulus was increased >70%. The Flexure modulus is 6 to 38.9 GPa and tensile modulus is 3.5 to19.52 GPa in tension. Tensile modulus is derived to newly formed PMMA and PLLA specimen by tensile testing machine.

## IV. TESTING

**4.1 Mobile wear**

The definition of wear may include loss of dimension from plastic deformation if it is originated at the interface between two sliding surfaces. Wear is related to interactions between

surfaces and more specifically the removal and deformation of material on a surface as a result of mechanical action of the opposite surface. The need for relative motion between two surfaces and initial mechanical contact between asperities is an important distinction between mechanical wear compared to other processes with similar outcomes. Some commonly referred to wear mechanisms (or processes) include:

1. Adhesive wear
2. Abrasive wear
3. Surface fatigue

4. Fretting wear. 5. Erosive wear. Knee joint occurs **abrasive wear**. Abrasive wear occurs when a hard rough surface slides across a softer surface. Wear comes in different forms -two types of wear are recognized: **Linear wear:** which is the measurement of rate and distance the metal component penetrates. **"Volumetric wear":** which is calculation of the volume of lost polyethylene and is proportional to the penetration rate and the area of contact. Conduct stress is increasing simultaneously wear is also increasing. Medial side wear is more than Lateral side wear. It is shown in Fig.20.

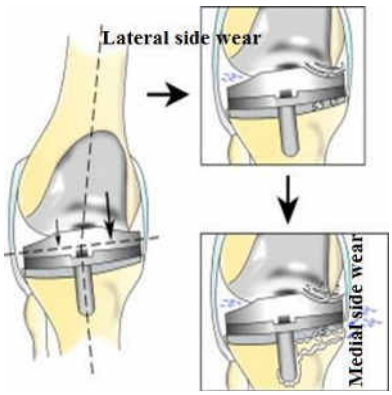


**Fig.20: Lateral and Medial side wear.**

### 4.2 Knee simulator

A single-station knee simulator was used to test the failure modes in the prosthesis. The knee simulator consists of an axial load generator using coil springs and a rotary drive mechanism which provides the articulation. The prostheses are tested in an inverted position, with the femoral component fixed in the base with dental acrylic and the tibial bearing on top facing downwards. A push rod from the rotary drive oscillates the tibial component through a range of flexion. The axial load is activated as the tibial bearing is pushed up over the contour of Loads were changed by using springs with different spring constants and by adjusting the position of the spring reaction framework. The single station Knee simulator is shown in Fig.21.

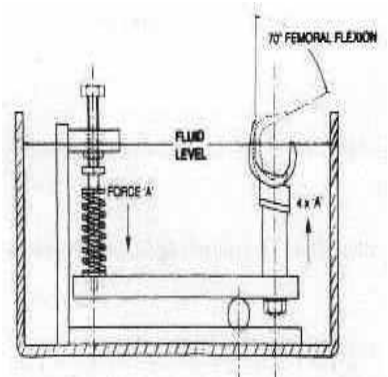


**Fig.21: Single station Knee simulator.**

Axial loads in this study ranged from 778 to 2000 N (175–450 lb). The range of flexion could be adjusted by changing the initial degree of flexion of the femoral component and the stroke amplitude of the drive rod. All tests were run with a flexion range of 0–35°. Lubrication between the components was provided by a bath of distilled water. Knee wear angles are flexion and extension angles at a $0^0$ to $120^0$. The following figures are given that Knee wear angles (Fig.22).

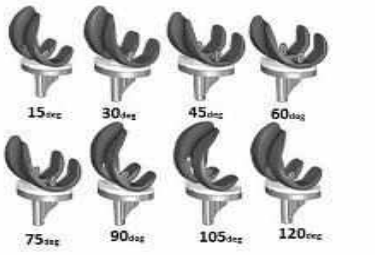


**Fig.22: Wear angles at $15^0$ of intervals.**

### 4.3 Wear capacity of polyethylene

The delamination failure in vivo. Implanted polyethylene components are sterilized and undergo subsequent ageing for some in vivo duration, at least before delamination occurs. Polyethylene wear is shown in fig.23.

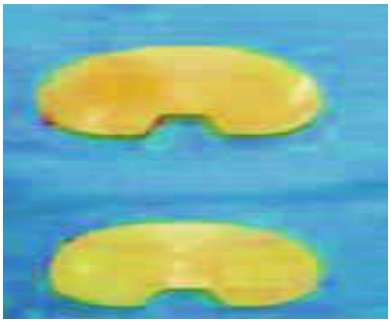

**Fig.23: Wear specimen of polyethylene by wear test.**

The knee simulation tests are resulted in polyethylene implant.

| MILLION CYCLES | MEDIAL | LATERAL |
|---|---|---|
| 3 MILLION CYCLES | 0.43mm | 0.38mm |
| 5 MILLION CYCLES | 0.85mm | 0.80mm |
| 11 MILLION CYCLES | 1 mm | 1 mm |

### 4.4 Wear capacity of newly formed PMMA and PLLA of copolymer

Copolymer is carried on wear simulation tester of single Knee tester. The knee simulation tests are resulted in PMMA with PLLA of copolymer implant. The sample wear specimen is shown in fig.24.

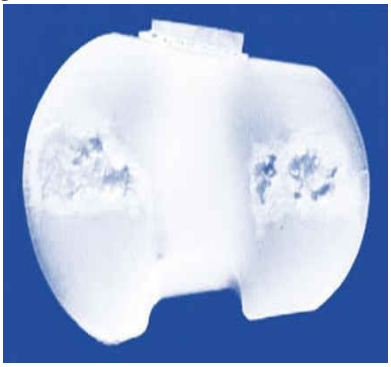

**Fig.24: Wear specimen of combination of PMMA with PLLA.**

| MILLION CYCLES | MEDIAL | LATERAL |
|---|---|---|
| 3 MILLION CYCLES | 0.1mm | 0.05mm |
| 5 MILLION CYCLES | 0.15mm | 0.1mm |
| 11 MILLION CYCLES | 0.25mm | 0.2mm |

**4.5 Knee simulation for Fixed vs. Rotating mobile bearing**

Already existing mobile bearing is wearing higher than comparing with newly rotating mobile bearing. The comparison is shown in fig.25.

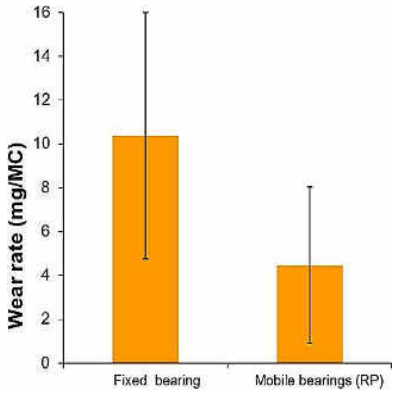


**Fig.25: Wear rate comparison between Fixed and Mobile bearing.**

## V. MODELLING

5.1 Modelling of the Existing mobile bearing

The existing mobile bearing size is shown in fig.26.

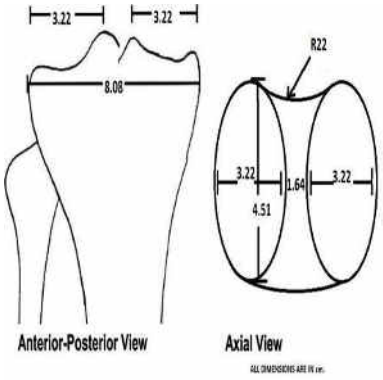


Fig.26: The existing Mobile bearing size.

It has same in size of both sides and it has screwed and bolted joint in fixed joint. The modelling of existing mobile bearing is shown in fig.27.

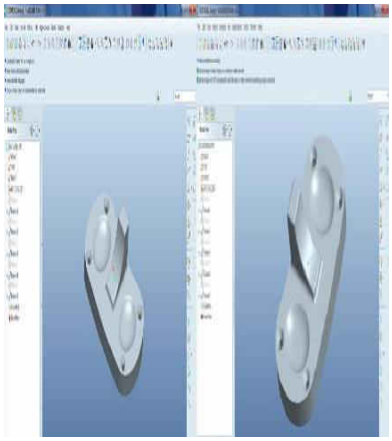

Fig.27: Existing mobile bearing 3D models by PRO-E.

5.2 Modelling of the modifying mobile bearing

The modifying mobile bearing size is shown in fig.28.

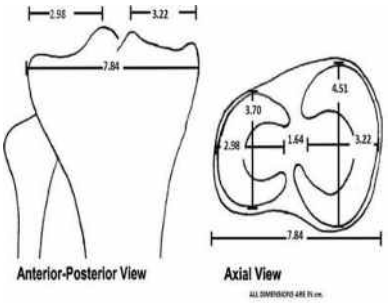


Fig.28: New mobile bearing size

It has different size in both sides. Lateral side is smaller than Medial side. It has slightly rotation at an angle of $3^0$ to $5^0$. The modelling of Modifying mobile bearing is shown in fig.29

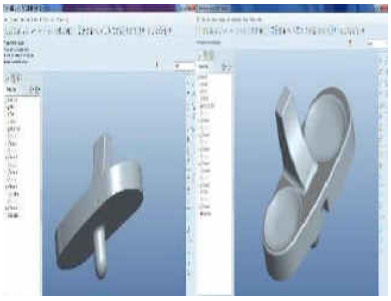

Fig.29: 3D PRO-E models of Modifying Mobile bearing.

## VI. MESH

6.1 Meshing of the existing mobile bearing

The existing mobile bearing mesh size is controlled by Mesh control through the sizing and refinement on 6668 nodes and 32240 elements (Fig.30).

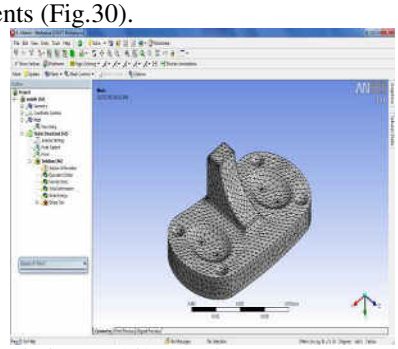

Fig.30: The existing mobile bearing 3D meshing by ANSYS.

6.2 Meshing of the modifying mobile bearing

The modified mobile bearing mesh size is controlled by Mesh control through the sizing and refinement on 68523 nodes and 42597 elements (Fig.31).

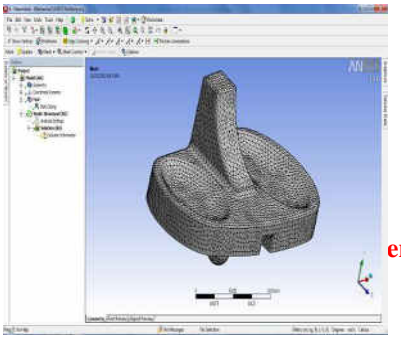

Fig.31: The modified mobile bearing 3D meshing by ANSYS.

## VII. ANALYSIS

7.1 Analysis of the existing mobile bearing

Axial loads in this study ranged from 778 to 2000 N (175–450 lb). Maximum load of 2000N is calculated from various standing, sitting, running, jumping and gym in position. Fig. 32 shows load and supports.

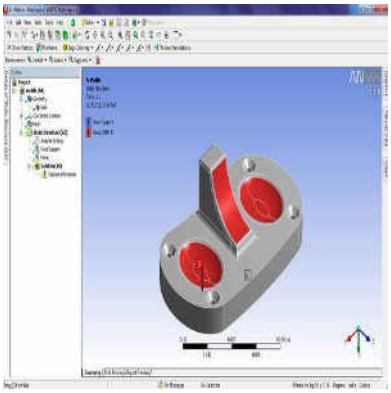

Fig.32: The existing mobile bearing load and support by ANSYS.

*7.1.1 Analysis on Equivalent (von-misses) stress*

The existing mobile bearing von-misses stress is calculated by structural analysis on maximum stress 3.6786 MPa (Fig.33).

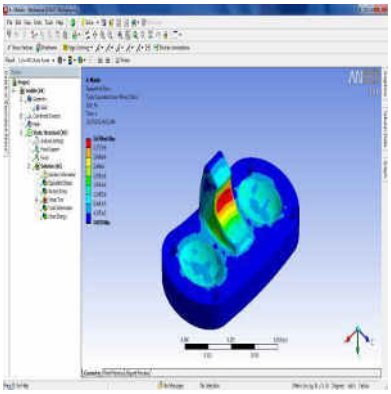

Fig.33: The existing mobile bearing analysis on Equivalent (von-misses) stress.

*7.1.2 Analysis on Normal (X-axis) stress*

The existing mobile bearing Normal stress is calculated by structural analysis on maximum stress 0.86637 MPa (Fig.34).

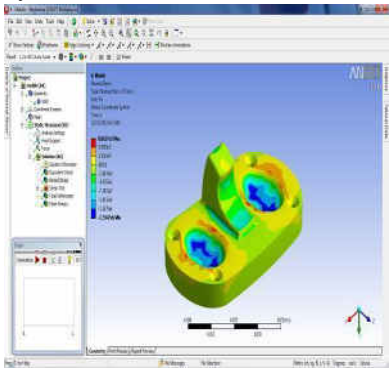

Fig.34: The existing mobile bearing analysis on Normal stress.

*7.1.3 Analysis on Maximum principle stress*

The existing mobile bearing Maximum principle stress is calculated by structural analysis on maximum stress 2.1661 MPa (Fig.35).

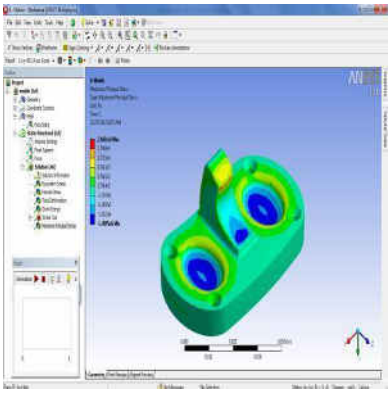

Fig.35: The existing mobile bearing analysis on Maximum principle stress.

*7.1.4 Analysis on Total deformation*

The existing mobile bearing Total deformation is calculated by structural analysis on maximum deformation 0.051381 mm (Fig.36).

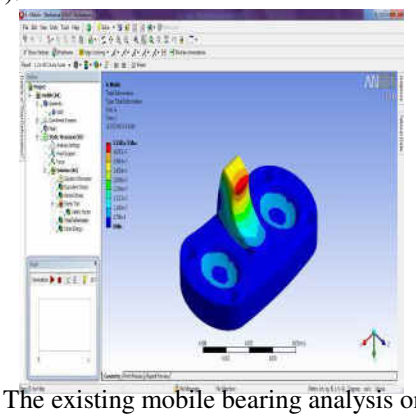

Fig.36: The existing mobile bearing analysis on Total deformation.

*7.1.5 Analysis on Strain energy*

The existing mobile bearing Strain energy is calculated by structural analysis on maximum Strain energy 7.4818e-5 J (Fig.37).

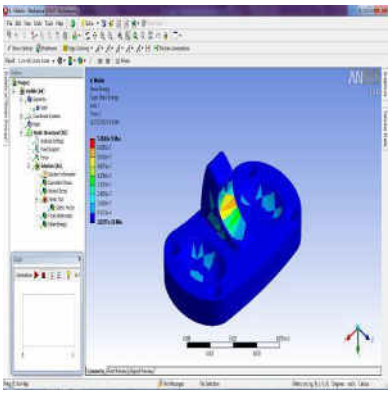

Fig.37: The existing mobile bearing analysis on Strain energy.

7.2 Analysis of the modifying mobile bearing

Axial loads in this study ranged from 778 to 2000 N (175–450 lb). Maximum load of 2000N is calculated from various standing, sitting, running, jumping and gym in position. Fig. 38 shows load and supports.

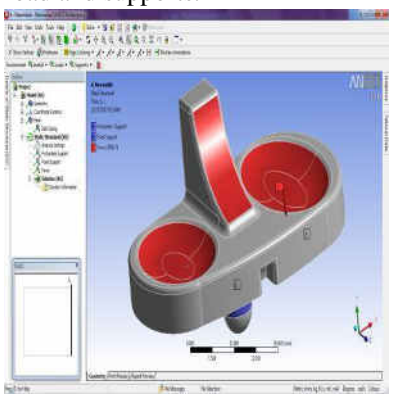

Fig.38: The modified mobile bearing load and support by ANSYS.

*7.2.1 Analysis on Equivalent (von-misses) stress*

The modified mobile bearing von-misses stress is calculated by structural analysis on maximum stress 2.3316 MPa (Fig.39).

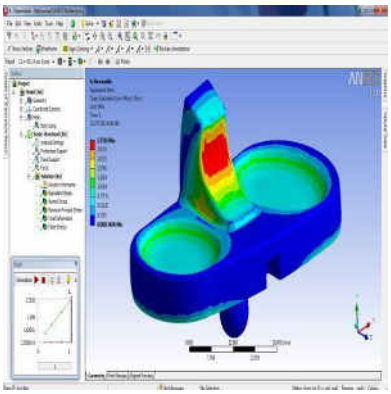

Fig.39: The modified mobile bearing analysis on Equivalent (von-misses) stress.

*7.2.2 Analysis on Normal (X-axis) stress*

The modified mobile bearing Normal stress is calculated by structural analysis on maximum stress 0.71861 MPa (Fig.40).

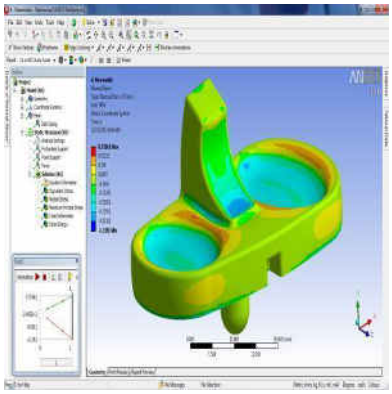

Fig.40: The modified mobile bearing analysis on Normal stress.

*7.2.3 Analysis on Maximum principle stress*

The modified mobile bearing Maximum principle stress is calculated by structural analysis on maximum stress 1.1937 MPa (Fig.41).

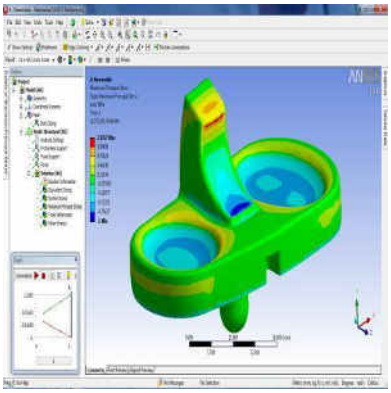

Fig.41: The modified mobile bearing analysis on Maximum principle stress.

*7.2.4 Analysis on Total deformation*

The modified mobile bearing Total deformation is calculated by structural analysis on maximum deformation 0.027808 mm (Fig.42).

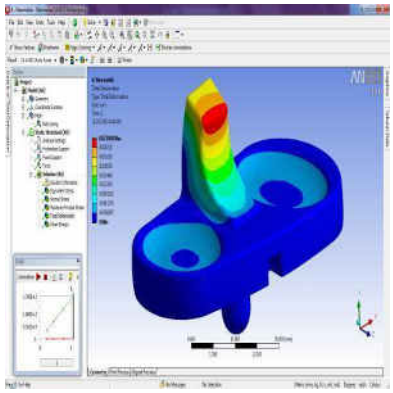

Fig.42: The modified mobile bearing analysis on Total deformation.

*7.2.5 Analysis on Strain energy*

The modified mobile bearing Strain energy is calculated by structural analysis on maximum Strain energy 0.0021203 mJ (Fig.43).

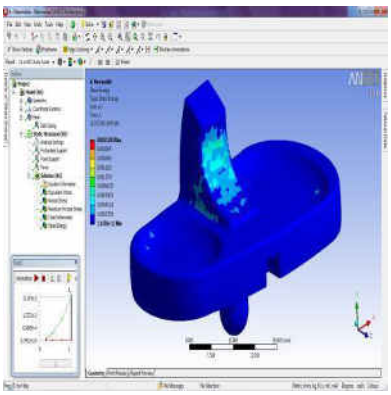

Fig.43: The modified mobile bearing analysis on Strain energy.

## CONCLUSION

### 8.1 Results

In this investigation is carried on few important Artificial Knee Joint models. The contact features of the different relative positions of Knee joints are learned from the patient's medical imaging (ex.: X-ray, MRI/CT) and Meniscus size is derived.

Wear capacity of existing Polyethylene and New bearing of PMMA/PLLA is obtained from wear test rig. New and existing Mobile bearing modeling is explained in this investigation by PRO-E, ANSYS software. Mobile bearing methodology of collection of data, selection of material, PRO-E modeling and ANSYS analysis of existing and new model mobile bearings are successfully achieved in this investigation.

### 8.2 The exist and new mobile bearing comparison

From above the new and existing mobile bearing analysis data's are given on minimum Equivalent (von-misses) stress, Normal stress, Maximum principle stress, Total deformation and suitable Strain energy comparing with polyethylene existing mobile bearing.

## ACKNOWLEDGEMENT

Investigation data's are collected from VEE CARE HOSPITAL- CHENNAI and VIKRAM MULTI SPECIALITY HOSPITAL – MADURAI.

## REFERENCES

[1]. P.J. Lemstra, R. Kirschbaum, T. Ohta, H. Yasuda, (2010), "*Developments in Oriented Polymers-2",* I.M. Ward, (Ed.), (1987), Elseviers, *"Applied Science*", London, 39.

[2]. M. Lammers, E.A. Klop, M.G. Nordholt, D.J. Sikkema, "*Polymer",* 39, (1998), 5999.

[3]. M. Lammers, Ph-D Thesis, ETH Zürich, (1998), "*Polymer,"* ch. 6

[4]. T. Nishino, H. Okhubo, K.J. Nakamae, Macomol, "*Sci., Phys.,"* B31, (1992), 191.

[5]. E.K. Nakamae, T. Nishino, "*Advances in X-ray analysis"*, (1992), 545.7. In Vivo. *"Business and medicine report"*, April 1995.

[6]. "ASTM Designation F-648-84 Standard Specification for Ultra-high-molecular-weight Polyethylene Powder and Fabricated Form for

[7]. Surgical Implants"- Annual book of ASTM Standards, 1994 (American Society of Testing and Materials, Philadelphia, Pennsylvania).

[8]. Hood, R. W., Wright, T. M. and Burstein, A. H. (1983), *"Retrieval analysis of total knee prostheses: a method and its application to 48 total condylar prostheses"*, J. Biomed. Mater.Res.1983, 17, 829.

[9]. Landy, M. M. and Walker, P. S. (1999), *"wear of ultra-high- molecular-weight polyethylene components of 90 retrieved knee prostheses".*

[10].[Treharne, R. W., Young, R. W. and Young, S. R. (1981), *"wear of artificial jointMaterials III: simulation of the knee joint using a computer controlled system".*

[11].Feehan, J. P. (1990), *"A multi-axis knee wear tester: design and preliminary results.MS thesis*",Thayer School of Engineering, DartmouthCollege, 1990.

[12].Van Jonbergen HPW, Werkman DM,Barnaart LF, van Kampen A(2010), *" Long-termoutcomes of patellofemoral arthroplasty"*, Arthroplasty 2010, 25:1066

[13].Essinger, J.R., Leyvraz, P.F., Heegard, J.H., 1229-1241, (1989), "*A mathematical model for the evaluation of the behaviour during flexion of condylar-type knee prosthesis",* Journal of Biomechanics, 22(11-12).Garg, A., Walker, P.S.,(1990),

[14]. *"Prediction of total knee motion using a three-dimensional computer graphics model*", Journal of Biomechanics, 23(1), 45-58.Sathasivam, S., Walker, P.S.,(1997), *"A computer model with surface friction for the prediction of total knee kinematics"*, Journal of Biomechanics. Pandy,

[15]. M.G., Sasaki, K., (1998), *"A three-dimensional musculoskeletal model of the human knee joint. Part 2: analysis of ligament function"*, Computer Methods in Biomechanics and Biomedical Engineering, 1(4), 265–283, 1998.